https://rbgeomorfologia.org.br/
ISSN 2236-5664

Revista Brasileira de Geomorfologia

v. 27, nº 1 (2026)

https://dx.doi.org/10.20502/rbg.v27i1.2683

Research Paper

Hydrosedimentary Dynamics in the Confluence of the Beni and Mamoré Rivers

Dinâmica hidrossedimentar na confluência dos rios Beni e Mamoré

Ednaldo Bras Severo [1], Rogério Ribeiro Marinho [2], Jean-Michel Martinez [3], Naziano Pantoja Filizola [4], Henrique Llacer Roig [5], Keila Aniceto [6], William Santini [7], Diogo Olivetti [8], André Zumak [9], Osmair Santos [10], Matheus Silveira de Queiroz [11], Camila Souto [12], Daniel Fernandes [13]

[1] Universidade Federal do Amazonas, Programa de Pós-graduação em Geografia, Manaus, Brasil. edsevero.geo@gmail.com
ORCID: https://orcid.org/0000-0002-9148-5570

[2] Universidade Federal do Amazonas, Programa de Pós-graduação em Geografia, Manaus, Brasil. rogeo@ufam.edu.br
ORCID: https://orcid.org/0000-0001-5219-8635

[3] Institut de Recherche pour le D´eveloppement (IRD) / Centre National de la Recherche Scientifique (CNRS) / Université Toulouse 3, Géosciences Environnement Toulouse (GET), Toulouse, France. jean-michel.martinez@ird.fr
ORCID: https://orcid.org/0000-0003-3281-8512

[4] Universidade Federal do Amazonas, Programa de Pós-graduação em Geociências, Manaus, Brasil. nazianofilizola@ufam.edu.br
ORCID: https://orcid.org/0000-0001-7285-7220

[5] Universidade de Brasília, Programa de Pós-graduação em Geociências Aplicadas e Geodinâmica, Brasília, Brasil. roig@unb.br
ORCID: https://orcid.org/0000-0002-9180-3081

[6] Universidade Federal do Amazonas, Programa de Pós-graduação em Geociências, Manaus, Brasil. keilaniceto@ufam.edu.br
ORCID: https://orcid.org/0000-0001-8258-1328

[7] Institut de Recherche pour le D´eveloppement (IRD) / Centre National de la Recherche Scientifique (CNRS) / Université Toulouse 3, Géosciences Environnement Toulouse (GET), Toulouse, France. william.santini@ird.fr
ORCID: https://orcid.org/0000-0003-0098-9755

[8] Universidade Federal de Alfenas, Instituto de Ciências da Natureza, Alfenas, Brasil. diogo.olivetti@unifal-mg.edu.br
ORCID: https://orcid.org/0000-0002-2491-6000

[9] Instituto de Desenvolvimento Sustentável Mamirauá, Tefé, Brasil. andre_zumak@yahoo.com.br
ORCID: https://orcid.org/0000-0003-4000-4527

[10] Universidade de Brasília, Programa de Pós-graduação em Geociências Aplicadas e Geodinâmica, Brasília, Brasil. osmairsf@gmail.com
ORCID: https://orcid.org/0009-0007-7424-8585

[11] Universidade Federal do Amazonas, Programa de Pós-graduação em Geografia, Manaus, Brasil. matheussilveiradequeiroz@gmail.com
ORCID: https://orcid.org/0000-0001-8722-7715

[12] Jirau Energia, Porto Velho, Brasil. camila.souto@jirauenergia.com.br.
ORCID: https://orcid.org/0009-0001-4424-5646

[13] Jirau Energia, Porto Velho, Brasil. daniel.fernandes@jirauenergia.com.br
ORCID: https://orcid.org/0009-0001-7565-2180

Received: 24/02/2025; Accepted: 18/02/2026; Published: 28/03/2026

Abstract: This study analyzed hydrosedimentary dynamics at the confluence of the Beni and Mamoré rivers, the main source rivers of the Madeira River, the largest tributary of the Amazon River. Thirteen field campaigns were conducted between March 2021 and April 2022 at four cross-sections, complemented by historical data from the HYBAM Observatory. The results

showed clear contrasts between the tributary rivers: mean suspended sediment concentrations (SSC) were 639 mg.L^{-1} in the Beni and 218 mg.L^{-1} in the Mamoré, with specific yields of 2.07 and 0.34 ton.km^{-2}.yr^{-1}, respectively. The Madeira River exhibited intermediate SSC values (357–371 mg.L^{-1}). During high-water conditions, vertical SSC stratification was more pronounced in the Mamoré and Madeira rivers. The sediment budget indicated a 15% deficit downstream of the confluence, corresponding to the retention of approximately 40 million tons over a 220 km reach. Downstream of this confluence lies the Jirau hydropower dam, whose dam may influence the study reach. Together, the Beni and Mamoré rivers contribute about 291 million tons of suspended sediment annually to the Madeira River, confirming their strategic role in the Amazon sediment budget and providing a basis for sustainable management of this watershed's resources.

Keywords: Amazon Basin; Suspended Sediment Concentration; Madeira River; Hydropower dam.

Resumo: Este estudo analisou a dinâmica hidrossedimentar na confluência dos rios Beni e Mamoré, principais formadores do rio madeira, que por sua vez é o maior afluente do rio Amazonas. Nesta região, foram realizadas 13 campanhas entre março de 2021 e abril de 2022 em quatro seções, complementadas por dados históricos do Observatório HYBAM. Os resultados revelaram diferenças significativas entre os rios formadores: concentrações médias de material em suspensão (MES) de 639 mg.L^{-1}, no Beni, e de 218 mg.L^{-1}, no Mamoré, com produção específica de 2,07 e 0,34 ton.km^{-2}.ano^{-1}, respectivamente. O rio Madeira apresentou concentrações intermediárias (357-371 mg.L^{-1}). Durante águas altas, a estratificação do MES em profundidade foi mais pronunciada nos rios Mamoré e no Madeira. O balanço sedimentar realizado evidenciou déficit de 15% a jusante da confluência. Este percentual representa uma retenção de 40 milhões de toneladas ao longo de 220 km. A jusante desta mesma confluência encontra-se o reservatório da Usina Hidrelétrica de Jirau, cuja barragem gera influência no trecho em questão. Os rios Beni e Mamoré, juntos, contribuem com 291 milhões de toneladas anuais para o rio Madeira, confirmando seu papel estratégico no balanço sedimentar amazônico e fornecendo base para gestão sustentável dos recursos desta bacia hidrográfica.

Palavras-chave: Bacia Amazônica; Concentração do Sedimento Suspenso; Rio Madeira, Hidrelétrica.

1. Introduction

The Amazon basin contains four of the ten largest rivers in the world in terms of mean annual water discharge: Amazon, Negro, Madeira, and Japurá Rivers (Latrubesse; Stevaux; Sinha, 2005). The Madeira River stands out as the second largest contributor in terms of water volume and the main supplier of sediments (approximately 50%) to the Amazon River (Rivera et al., 2019, 2021; Vauchel et al., 2017). In addition to its hydrological relevance, it constitutes an important national waterway, commercially integrating the North and Central-West regions of Brazil (DNIT, 2024).

The Beni and Mamoré rivers, which constitute the main tributaries forming the Madeira River (Lopes; Magalhães, 2018; Severo et al., 2024), originate in the Andean region and have a mean annual water discharge of 9,083 m^3.s^{-1} and 7,114 m^3.s^{-1}, respectively. Together they transport approximately 430×10^6 ton.year^{-1} of suspended sediment, directly conditioning the hydrosedimentary dynamics of the Madeira River (Vauchel et al., 2017).

In recent decades, the Beni and Mamoré river basins have undergone intense anthropogenic transformations (Souza et al., 2022). Deforestation, agricultural expansion, and urbanization resulted in the loss of 2.44% of natural cover in the Beni basin and 12.62% in the Mamoré basin between 1990 and 2020, while agricultural and infrastructure areas increased by 193.64% and 250.36%, respectively (Severo; Marinho, 2023). Concomitantly, the region presents increasing climatic variability, with changes in precipitation patterns and intensification of extreme climatic events (Espinoza et al., 2019).

These anthropogenic modifications and recent climate variability have altered the hydrological regime of the rivers and may intensify erosive and depositional processes in different fluvial systems (Li et al., 2024; Queiroz et al., 2025). In the case of the Madeira River, Rivera et al. (2019, 2021) identified a reduction in sediment transport at stations in the upper Madeira Basin, including Cachuela Esperanza (Beni River), Guayaramerín (Mamoré River), and Porto Velho (Madeira River), the latter influenced by the dams of the Madeira River Hydroelectric Complex. In the same reach, Latrubesse et al. (2017) identified a reduction of ~20% in the mean annual surface suspended sediment concentration downstream of the Santo Antônio Dam, in the Porto Velho region.

Although studies have identified trends of reduced sediment transport in isolated stations of the Madeira basin, it remains unclear how these changes specifically manifest themselves in the hydrosedimentary dynamics of the Beni-Mamoré confluence region. In particular, the magnitude of the integrated impacts of land-use changes and climate variability on suspended sediment transport and water discharge at this strategic confluence is not adequately known (Severo; Marinho, 2023). This gap limits the understanding of the hydrosedimentological processes essential for the management of the Madeira River waterway and for the assessment of the impacts of hydraulic infrastructures on large tropical rivers.

This work aims to analyze the hydro-sedimentological dynamics at the confluence of the Beni and Mamoré rivers, evaluating the regimes of suspended sediment concentration (SSC), water discharge (Q), and solid discharge (Qs), based on field data and historical series from hydrometric stations. The study provides novel hydrosedimentological data and proposes a regional sediment balance.

Based on the context presented, the following hypotheses are formulated: (i) there are significant differences in sediment and water transport regimes between the sections of the Beni-Mamoré confluence and the Madeira River downstream, related to the specific geomorphological and hydrodynamic characteristics of each reach; (ii) the presence of hydraulic structures downstream (e.g., Jirau hydropower dam) alters the sediment balance downstream of the confluence, promoting retention of particulate matter; (iii) the patterns of suspended sediment concentration show distinct seasonal and vertical variability between the Beni, Mamoré, and Madeira rivers, reflecting their different geological origins and transport conditions.

2. Study Area

The study area is located at the confluence of the Beni and Mamoré Rivers and in the subsequent 220 km reach of the Madeira River, in the state of Rondônia, on the Brazil-Bolivia border (Figure 1). The Beni Basin covers 282,000 km² in Bolivian (61%) and Peruvian (39%) territory, while the Mamoré Basin has 636,000 km² distributed between Bolivia (81%) and Brazil (19%). (Severo et al., 2024).

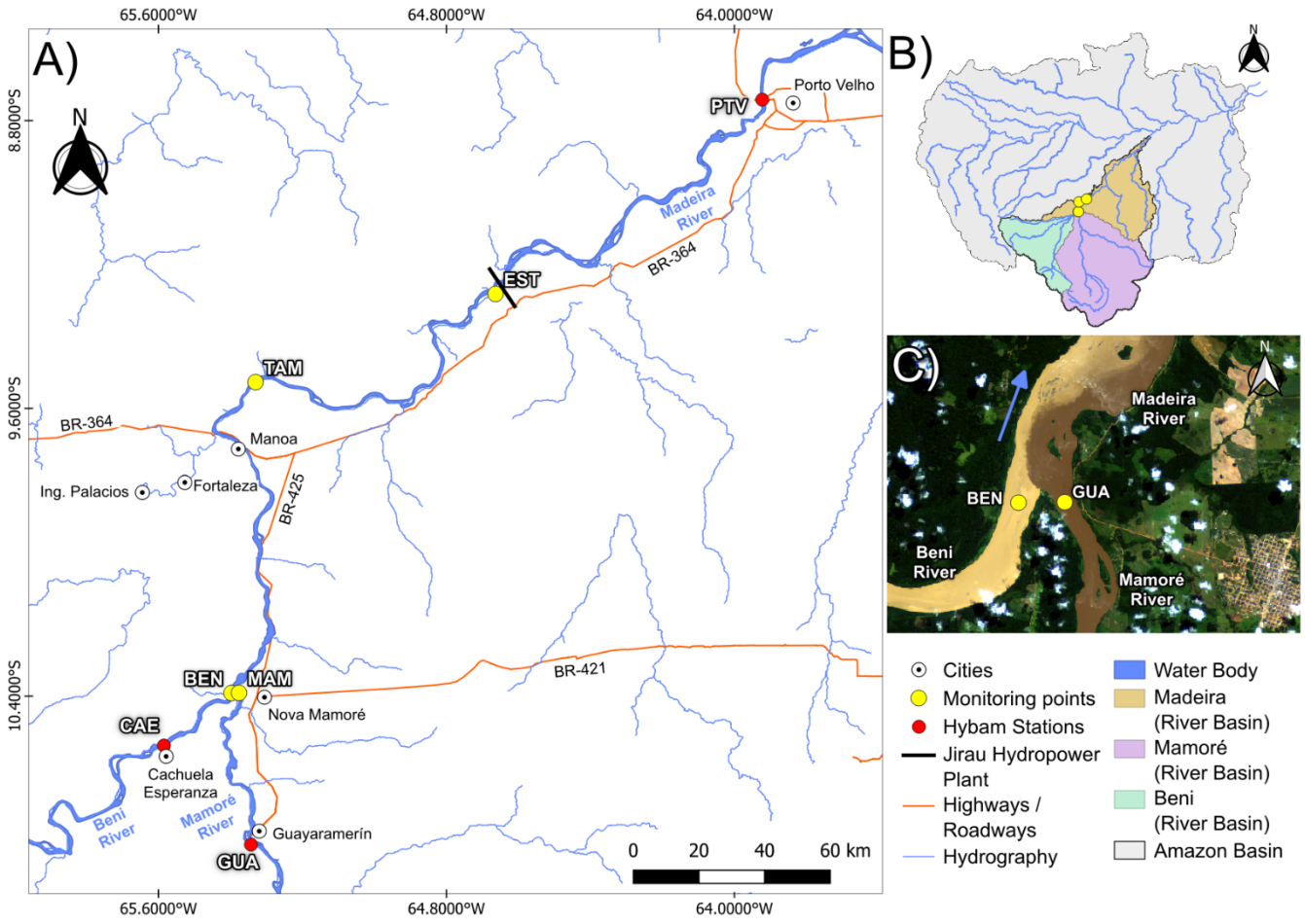

Figure 1. Study area at the Beni-Mamoré confluence and Madeira River. A) Monitoring points: BEN (Beni River), CAE (Cachuela Esperanza), EST (Station), GUA (Guayaramerín), MAM (Mamoré River), PTV (Porto Velho) and TAM (Tamborete). B) Location of sub-basins in the Amazon basin. C) Satellite image of the confluence (02/06/2021) with BEN and GUA stations.

The basins present a geological substrate characterized by Paleozoic metasedimentary and Mesozoic plutonic rocks, overlying the Proterozoic metamorphic basement associated with the Andes Mountains. Within this framework, the Andean orogeny began in the Cretaceous (≈145–66 Ma) and was associated with the formation of a foreland basin between the more intensely weathered Brazilian Shield and the Andean orogenic belt. This basin began to develop around 100 Ma, during the transition between the Lower and Upper Cretaceous, and remains active to the present, acting as an important area for the deposition of sediments from the Andes into the Madeira River basin. Estimates indicate that, in the southern Andean Piedmont and in the foreland basin, the mean deposition rate reaches approximately 210 Mt year^{-1} (Vauchel et al., 2017). The eastern portion of the basins is covered by extensive Quaternary cover composed of siliciclastic sediments (Alcárcel-Gutiérrez et al., 2023).

The studied reach is located on the edges of the Amazonian depositional basin, in direct contact with the Brazilian Shield, where the Madeira River becomes entrenched. This strategic geographical position, between the peri-Andean tectonic transition zone and the Amazonian plain, conditions the regional hydrosedimentary characteristics. The area integrates the geomorphological domain of the Plains and Wetlands of the Middle and Upper Guaporé, characterized by floodplains, meandering rivers and alluvial depositional systems (Souza Filho et al., 1999).

The region presents great climatic diversity, ranging from semi-arid areas in the Andes to reaches of dense forest on Paleozoic rocks (Guyot; Jouanneau; Wasson, 1999). The regional climate presents a well-defined seasonal pattern, with a mean annual rainfall of 1,900 mm in the Beni basin and 1,350 mm in the Mamoré basin (Figure 2). The rainy season is concentrated between January and March, followed by a dry season from April to August. The Beni, Mamoré, and Madeira rivers are classified as white-water rivers, with a multi-channel pattern and high sediment load (Latrubesse; Stevaux; Sinha, 2005; Sioli, 1984).

Water discharges exhibit strong seasonal variability, with peaks between March and April. In Cachuela Esperanza (Beni River), the water discharge varies from 2,946 m^3·s^{-1} in September to 18,286 m^3·s^{-1} in March. In Guayaramerín (Mamoré River), it oscillates between 1,635 m^3·s^{-1} in October and 15,552 m^3·s^{-1} in April. In the Madeira River (Porto Velho), the range varies from 4,672 m^3·s^{-1} in September to 36,139 m^3·s^{-1} in March, reflecting the integration of the hydrological regimes of its tributaries. Filizola and Guyot (2011) highlight that the water and solid flows of the Beni and Mamoré rivers are highly irregular, with large annual variations.

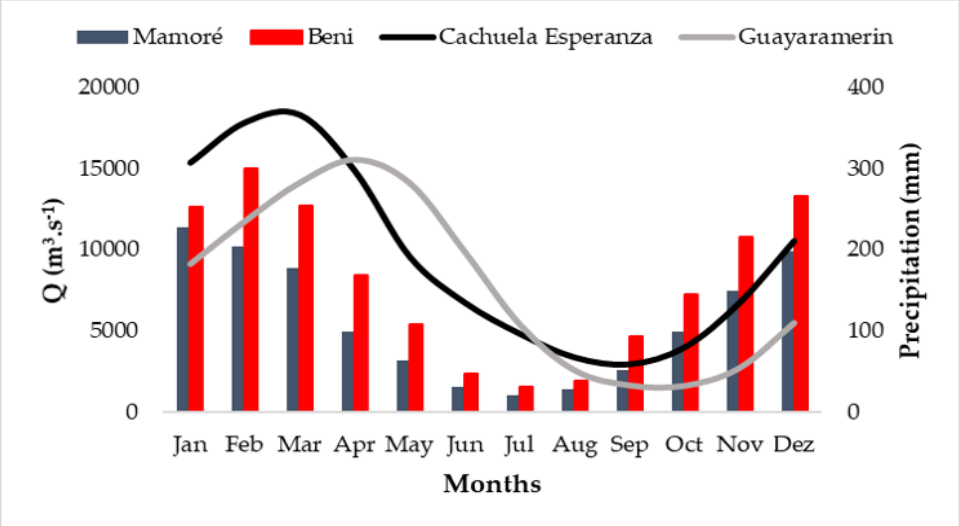

Figure 2. Mean monthly precipitation (bars) and water discharge (Q) regime in the Beni and Mamoré river basins. Precipitation data for the period 1990-2020 and water discharge (lines) from 1984 to 2020. Source: CHIRPS (2024); (HYBAM, 2024).

3. Materials and Methods

Thirteen hydrosedimentary sampling campaigns were conducted between March 2021 and April 2022 in reaches located in the Beni, Mamoré, and Madeira rivers upstream of the Jirau hydropower dam, complemented by historical series from the HYBAM Observatory (1980-2024). 500 ml water samples were collected at a depth of 20 cm at points 25%, 50%, and 75% of the channel width to determine the SSC.

To analyze the vertical variation of SSC, a bottom sampler was used at three points in the cross-section and at three different depths. All samples were sieved through a 63 μm mesh and processed at the Geochemistry Laboratory of the Federal University of Amazonas (UFAM) following the protocol HYBAM (2024) for determining the SSC concentration (in $mg.L^{-1}$), a procedure in line with recommendations for water quality monitoring and suspended sediment sampling disseminated within the GEMS/Water framework (Chapman, 1992).

Water Discharge (Q) and velocity (V) data were measured with an Acoustic Doppler Current Profiler (ADCP) model Rio Grande 600 kHz coupled to a Trimble R4 GNSS receiver. Two to four cross-sections were performed, using the means to determine the water discharge. Velocity vector and backscatter data from the ADCP signal were processed using the Velocity Mapping Tool - VMT software (Parsons et al., 2013).

The hydrosedimentological parameters of suspended sediment concentration (SSC), solid discharge (Qs), mean annual solid discharge (Qsa), and specific sediment yield were calculated using equations 1, 2, 3, and 4, respectively.

$$\mathrm{SSC} = \left((Pf - Pi) * \frac{1000000}{V} \right) \quad (1)$$

Where SSC ($mg.\ L^{-1}$) is the suspended sediment concentration, determined by the difference between the final weight (Pf) and initial weight (Pi) of the filters, multiplied by 1,000,000 (conversion factor) and divided by the filtrate volume (V).

$$Qs = Q\ x\ \mathrm{SSC}\ x\ 0.0864 \quad (2)$$

Where Qs is the mean solid discharge ($ton.day^{-1}$), Q is the water discharge of the section ($m^3.s^{-1}$), SSC is the suspended sediment concentration ($mg.L^{-1}$) and 0.0864 is a conversion factor.

$$Qsa = Qs\ x\ 365 \quad (3)$$

Where Qsa is the mean annual sediment transport in $tons.year^{-1}$.

$$Qsp = Qsa\ /\ Ab \quad (4)$$

Where Qsp is the specific sediment production ($ton/km^2.year$), Ab is the basin area, with values of 280,000 km^2 for the Beni River, 636,000 km^2 for the Mamoré River, and 959,000 km^2 for the Madeira River in the EST monitoring point.

The hysteresis loops were classified based on the direction (clockwise/counterclockwise) and shape of the SSC–Q trace over the analyzed period, following the typology and discussion of hysteresis classified by Jing et al., (2025).

The vertical variation in suspended sediment concentration (SSC) was synthesized by a stratification coefficient (SC), defined as the ratio between the mean SSC at depth (SSC_{prof}) and the SSC at the surface (SSC_{sup}):

$$\mathrm{SC} = \mathrm{SSC_{prof}} / \mathrm{SSC_{sup}} \quad (5)$$

Where SC is Stratification Coefficient for each campaign and section, SSC_{sup} corresponded to the concentration obtained at ~20 cm depth at points 25%, 50%, and 75% of the channel width (mean of these points). SSC_{prof} was calculated as the mean value of the samples obtained with the bottom sampler at the depths sampled at three points of the cross-section, excluding the surface sample. SC values close to 1 indicate low vertical stratification, while values >1 indicate higher relative concentration at depth. SC was used to compare the intensity of stratification between sections and campaigns.

The ADCP backscatter profiles were interpreted together with the SSC samples at depth to evaluate the spatial and vertical coherence of the observed patterns, as performed by Filizola and Guyot (2004). The mean velocity vectors were obtained by vertical integration (mean velocity in the water column) from the ADCP profiles, with

directional rotation/normalization relative to the main channel axis to allow comparisons between low and high-water periods.

The sediment balance was developed by the variation of Qsa between upstream and downstream reaches, where negative values indicate sediment retention and positive values indicate an increase in material between successive reaches, indicating erosive or depositional processes along the analyzed reach. Hysteresis loops between SSC and water discharge (Q) were used to identify the direction (clockwise or counterclockwise) and amplitude of temporal patterns, and the coefficient of determination (R^2) quantified the strength of the linear relationship between SSC and Q in each reach.

The HYBAM data from the Cachuela Esperanza station in the Beni River, Guayaramerin in the Mamoré River, and Porto Velho in the Madeira River (1980-2024) follow a standardized protocol with periodic collections at fixed stations, while the measurements in this research (2021-2022) involved 13 specific campaigns with greater spatial and vertical detail of the SSC distribution. This methodological difference was considered in the comparative analyses and interpretation of the results. The dataset was processed in a spreadsheet, allowing for the estimation of mean, minimum, and maximum values.

4. Results

4.1. The fluvial regime and sediment balance of the Beni, Mamoré, and Madeira rivers.

Analyses of mean monthly data (1980-2024) at the Guayaramerín (Mamoré River) and Cachuela Esperanza (Beni River) stations show counterclockwise hysteresis patterns between SSC and precipitation (Figures 3a and 3b). A time lag of approximately 0–1 month is observed between the monthly variations in SSC and precipitation: at Cachuela Esperanza, the precipitation and SSC peaks coincide in February (~0 months), while at Guayaramerín the precipitation peak occurs in January and the SSC peak in February (~1 month) (Figures 3a and 3b). During the low water, SSC decreases more slowly than precipitation, maintaining relatively high values in the first months of the dry season.

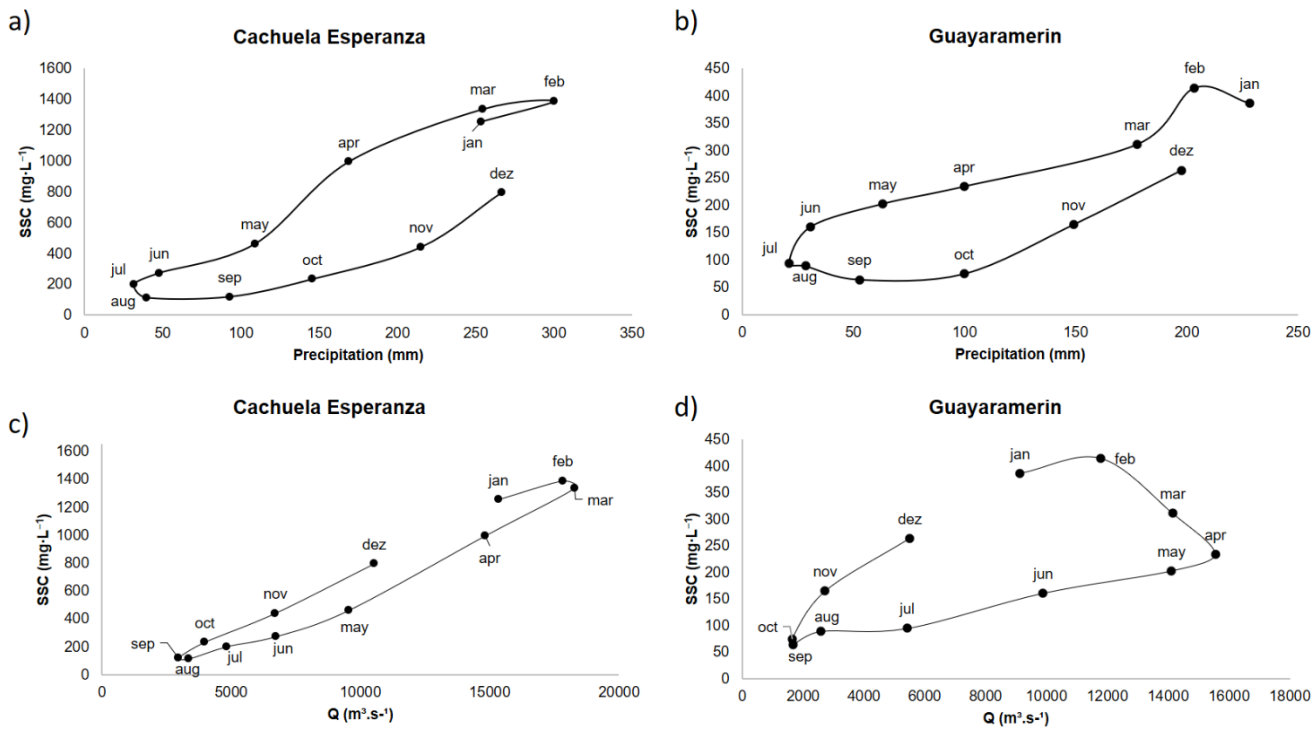

Figure 3. Mean monthly regime of SSC, precipitation (mm) and water discharge (Q) in the Beni and Mamoré river basins. Precipitation data for the period 1990-2020, SSC and water discharge from 1984 to 2020. Source: CHIRPS (2024); (HYBAM, 2024).

In the relationship between SSC and water discharge (Q), both sections exhibit clockwise hysteresis (Figures 3c and 3d). At Cachuela Esperanza, the SSC versus Q relationship is predominantly positive, but between May and November there is a strong variation in water discharge (>2,000 $m^3.s^{-1}$) with relatively stable SSC. At Guayaramerín, the hysteresis loop is more pronounced, showing clear differences between the water upwelling and downwelling regime, with SSC varying from 100-150 $mg.L^{-1}$ between April and August. In the Madeira River in Porto Velho, the SSC versus Q relationship (Figure 4) shows clockwise hysteresis like the upstream sections. Between April and July, high water discharge predominates with lower SSC concentrations, while from September to February, an almost linear relationship is observed between SSC and Q.

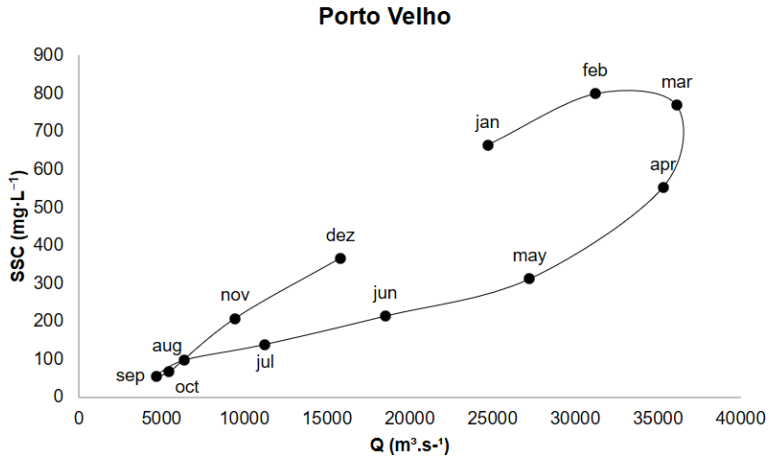

Figure 4. Mean monthly SSC versus mean monthly water discharge at the Porto Velho station in the Madeira River.

The mean daily solid discharge was 5.53×10^5 $ton.day^{-1}$ in Cachuela Esperanza (Beni River) and 1.36×10^5 $ton.day^{-1}$ in Guayaramerín (Mamoré River), resulting in an annual transport of approximately 2.02×10^8 and 0.50×10^8 $ton.year^{-1}$, respectively. In Porto Velho (Madeira River), a mean solid discharge of 6.10×10^5 $ton.day^{-1}$ and an annual transport of 2.23×10^8 $ton.year^{-1}$ were recorded (Table 1).

Table 1. Daily (Qs) and annual (Qsa) solid discharge of suspended material and observed variation of the sum of the Beni and Mamoré rivers downstream in Porto Velho (Δ).

Station	River	Qs ($ton.day^{-1}$)	Qsa ($ton.year^{-1}$)	Δ (%)
Cachuela Esperanza	Beni	$5.53x10^5$	$2.02x10^8$	-
Guayaramerín	Mamoré	$1.36x10^5$	$0.50x10^8$	-
Porto Velho	Madeira	$6.10x10^5$	$2.23x10^8$	-11,29

The hydrosedimentary balance in Porto Velho shows a deficit of 11.29% in relation to the sum of upstream discharges, representing a deposition of approximately 2.84×10^7 $ton.year^{-1}$ (7.77×10^4 $ton.day^{-1}$) in sediment transport along the analyzed reach.

4.2. Hydrosedimentary dynamics and SSC vertical variation

The hysteresis loops between suspended sediment concentration (SSC) and water discharge (Q) express differences in SSC, for the same Q value, between the rising and falling periods of the fluvial regime. Since the loops presented here were constructed from 13 sampling campaigns (2021–2022), comparisons with HYBAM products should consider differences in temporal scale and sampling frequency. In Figure 5, sections BEN, MAM, TAM, and EST show predominantly clockwise loops, with distinct shapes between the tributary rivers and the

Madeira River downstream. The coefficient of determination (R^2) between SSC–Q was moderate in BEN and MAM (0.66–0.67) and low in TAM (0.37), indicating greater dispersion of the SSC–Q relationship in this section.

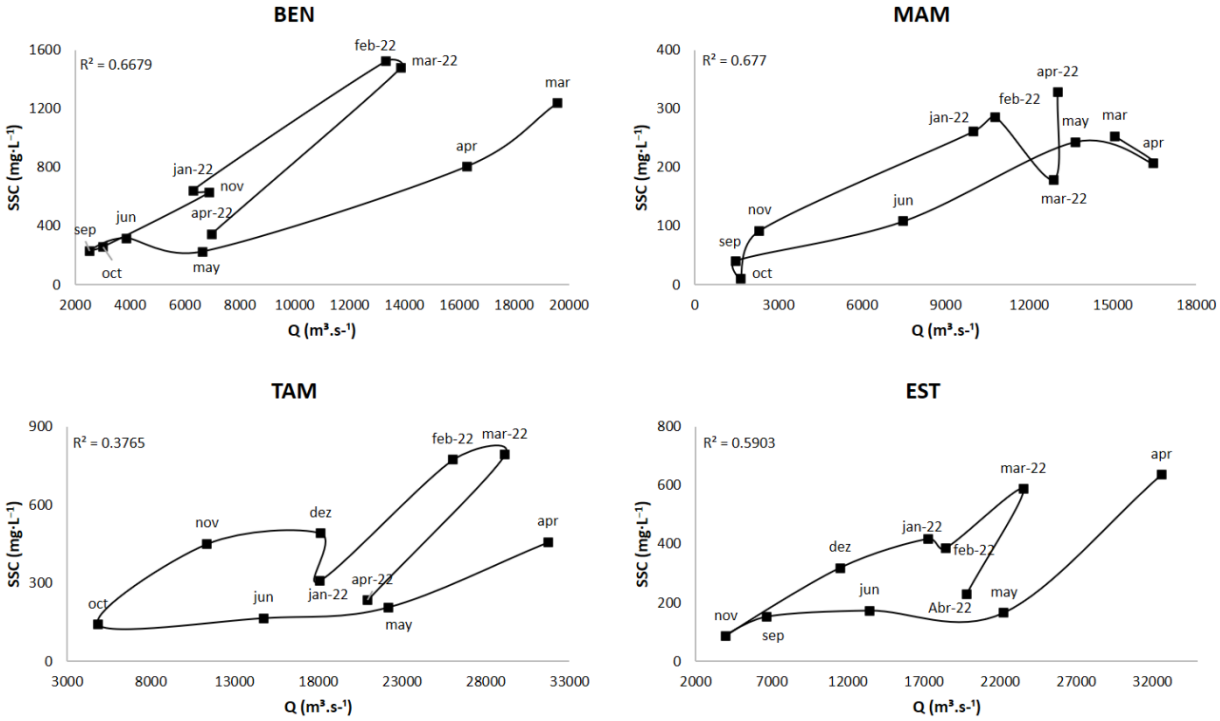

Figure 5. Hysteresis loops between SSC and water discharge (Q) in the BEN (Beni River), MAM (Mamoré River), TAM and EST (Madeira River) sections from March 2021 to April 2022. The graphs highlight the variations in SSC as a function of Q throughout the annual hydrological cycle.

In BEN, the greatest irregularities are concentrated in the low water field campaigns (June–October), with abrupt drops in SSC between successive campaigns and recovery in subsequent field campaigns. In MAM, the loop is more regular for most of the cycle, with a marked oscillation in March 2022. In TAM and EST, the points of the low-water field campaigns are at lower SSC levels than those observed in the high-water field campaigns. In addition, the May and November field campaigns show similar SSC values, although they correspond to different phases of the hydrological cycle.

The BEN section presented the highest mean SSC (639 $mg.L^{-1}$) and the highest specific yield (2.07 $ton.km^{-2}.year^{-1}$), even registering a lower water discharge (8,795 $m^3.s^{-1}$) compared to the other sections (Table 2). The MAM section, with a higher water discharge (10,531 $m^3.s^{-1}$), showed significantly lower SSC concentrations and specific yield (218 $mg.L^{-1}$ and 0.34 $ton.km^{-2}.year^{-1}$, respectively). In the TAM section, the highest mean velocity value (1.40 $m.s^{-1}$) occurred simultaneously with a water discharge of 20,716 $m^3.s^{-1}$ and an intermediate SSC concentration (371 $mg.L^{-1}$), resulting in an annual transport of approximately 257 million tons and a negative balance of 12% in relation to the total of the upstream sections. The EST section was characterized by the greatest channel width (1,134 m) and lowest velocity (0.73 $m.s^{-1}$), with SSC and Q values similar to those of the TAM section, but showing a new decrease in annual solid discharge (Qsa with a balance of -3%) and the lowest specific yield (0.24 $ton.km^{-2}.year^{-1}$) among all the sections evaluated.

Table 2. Characteristics of the four sections analyzed in the study. Mean values observed at the surface.

Section	River	Mean width (m)	Vel. ($m.s^{-1}$)	SSC ($mg.L^{-1}$)	Q ($m^3.s^{-1}$)	Qsa ($ton.year^{-1}$)	Balance (%)	Specific Yield ($ton.km^{-2}.ano^{-1}$)
BEN	Beni	859	1,03	639	8.795	212.207.962		2,07
MAM	Mamoré	632	1,01	218	10.531	79.663.303		0,34
TAM	Madeira	891	1,40	371	20.716	257.859.100	-12%	0,38
EST	Madeira	1134	0,73	357	20.146	251.342.233	-3%	0,24

Analysis of the vertical variation of SSC demonstrated distinct seasonal patterns among the monitored sections (Figure 6). In the BEN sections, the stratification coefficient (SC) reached maximum values of 2.9 in November and 2.3 in December 2021, decreasing to 1.7–1.8 in January–February 2022 and returning to high values during high water (2.4 in March and 2.0 in April). In the MAM sections, the SC was lower in November 2021 (1.1), progressively increased to 4.13 in March 2022, and decreased to 1.67 in April.

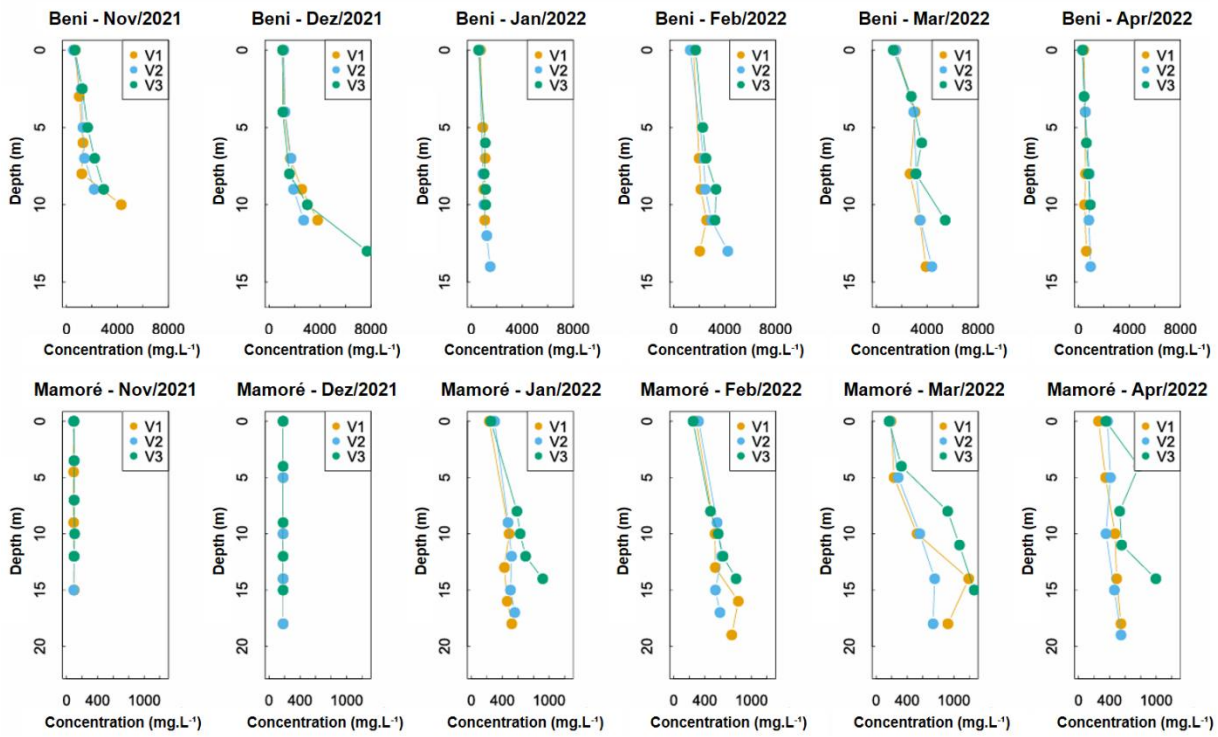

Figure 6. Vertical variation of SSC along three points (V1 – right bank, V2 – center of the channel, V3 – left bank) in the BEN (Beni River) and MAM (Mamoré River) sections, between November 2021 and April 2022.

In the Madeira River sections (Figure 7), the vertical variation of SSC was initially moderate, with a stratification coefficient (SC) of 1.37 (November) and 1.54 (December) in TAM. During high water (January), the SC increased to 2.81, remaining high in subsequent months (2.41 in March and 3.10 in April 2022), with a period mean of 2.2. In the EST section, the SC was lower, varying from 1.61 in January to 2.80 in March 2022, with a period mean of 1.9.

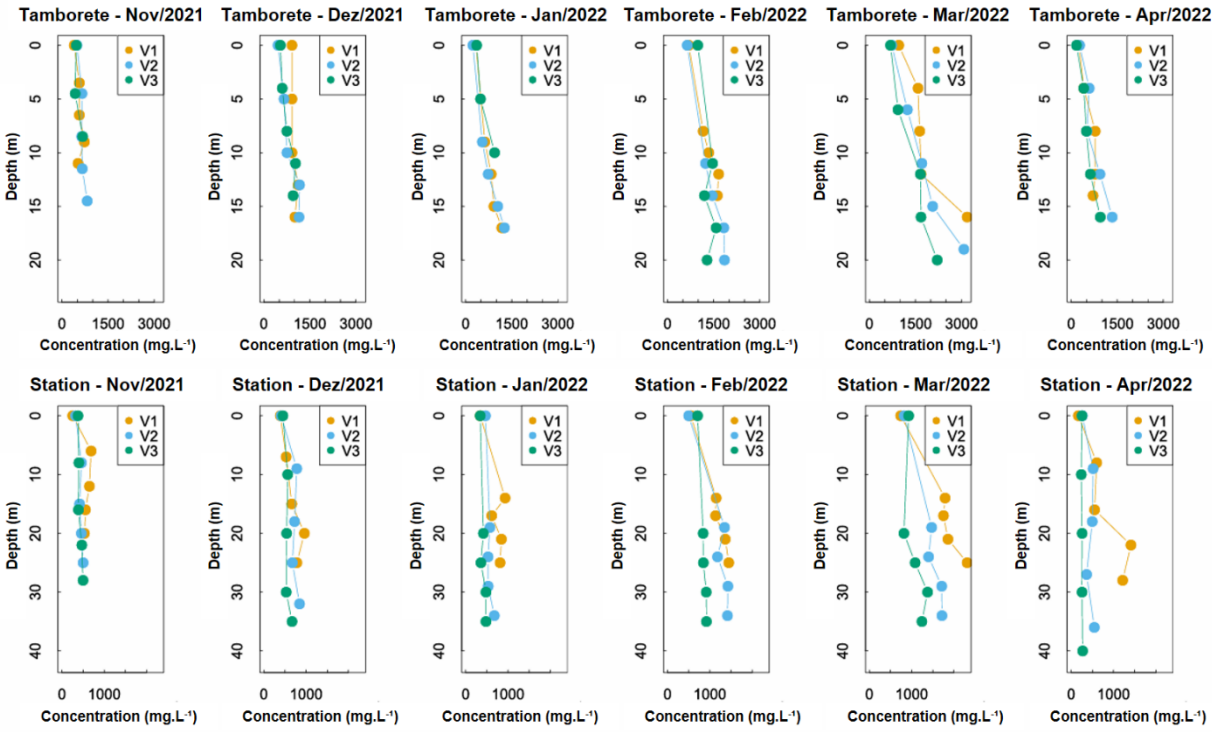

Figure 7. Variation in SSC with depth in the Tamborete (TAM) and Station (STN) sections of the Madeira River, from November 2021 to April 2022. Points V1, V2, and V3 correspond, respectively, to the right bank, center of the channel, and left bank.

The ADCP backscattered profiles confirm the vertical distribution patterns of SSC observed in the sampling analyses. During the low-water period in November 2021 (Figure 8), the BEN section showed the highest signal intensity in the center of the channel, with SSC concentrations ranging from 300 mg.L^{-1} to 900 mg.L^{-1}. The MAM section showed a more uniform distribution along the ADCP signal profile, with the left bank registering the highest concentrations (400-900 mg.L^{-1}). In the TAM section, the ADCP signal was most intense in the center of the channel between 10-14 m depth, where SSC showed high variation (300-1300 mg.L^{-1}). The EST section exhibited the highest intensity on the right bank, with concentrations reaching 1400 mg.L^{-1} between 20-30 m depth.

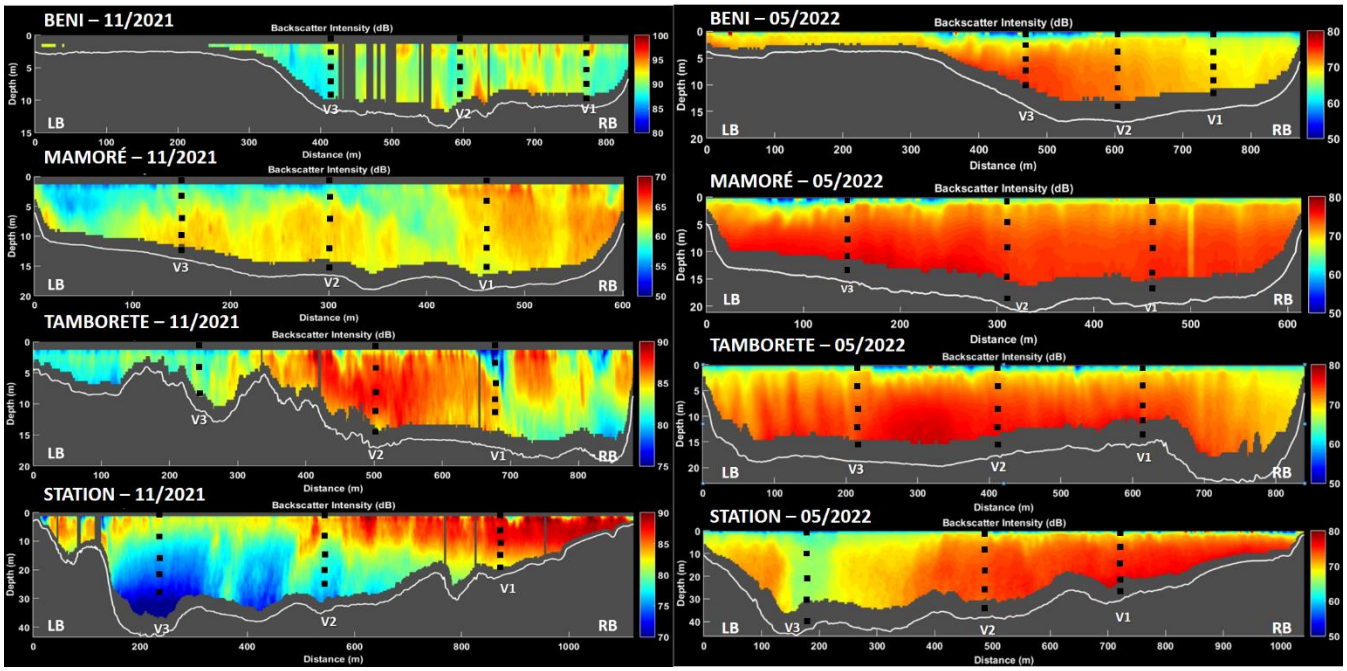

Figure 8. Cross-sectional profiles of the Beni, Mamoré, and Madeira rivers showing the variation in ADCP signal backscattering with depth in November and April of 2022 and 2021. LB: Left Bank. RB: Right Bank. Values are in decibels (dB). Dots indicate the sampling locations at depth.

During the high-water period in April 2022 (Figure 8), substantial changes were observed in the vertical distribution patterns. The BEN section showed a strong signal return on the right bank, confirming a higher concentration of SSC at depth in this region. In the MAM section, the signal intensified in the center of the channel and along the left bank, while the right bank recorded lower concentrations even in deeper zones. The TAM section exhibited high backscattering in the center of the channel, with concentrations ranging from 450 mg L^{-1} at the surface to 1000 mg L^{-1} at greater depths. The EST section showed higher intensity along the right bank, where concentrations of approximately 700 mg L^{-1} were recorded between 5 and 10 m depth, decreasing to lower values (around 500 mg L^{-1}) at greater depths.

The distribution of mean velocity vectors demonstrated significant hydrodynamic variations between hydrological periods and analyzed sections (Figure 9). During low water (November 2021), the EST section showed concentrated flow near the right bank with mean velocities of 0.41 $m.s^{-1}$ and orientation around 105°. The TAM section exhibited a distinct pattern, with more intense velocities (mean of 1.01 $m.s^{-1}$ and maximum of 1.40 $m.s^{-1}$) concentrated in the center of the river, oriented at 40°. At the Beni-Mamoré confluence, the Beni vectors reached a mean of 1.10 $m.s^{-1}$ concentrated along the right bank, while the Mamoré showed lower intensity (0.25 $m.s^{-1}$) predominating along the right bank.

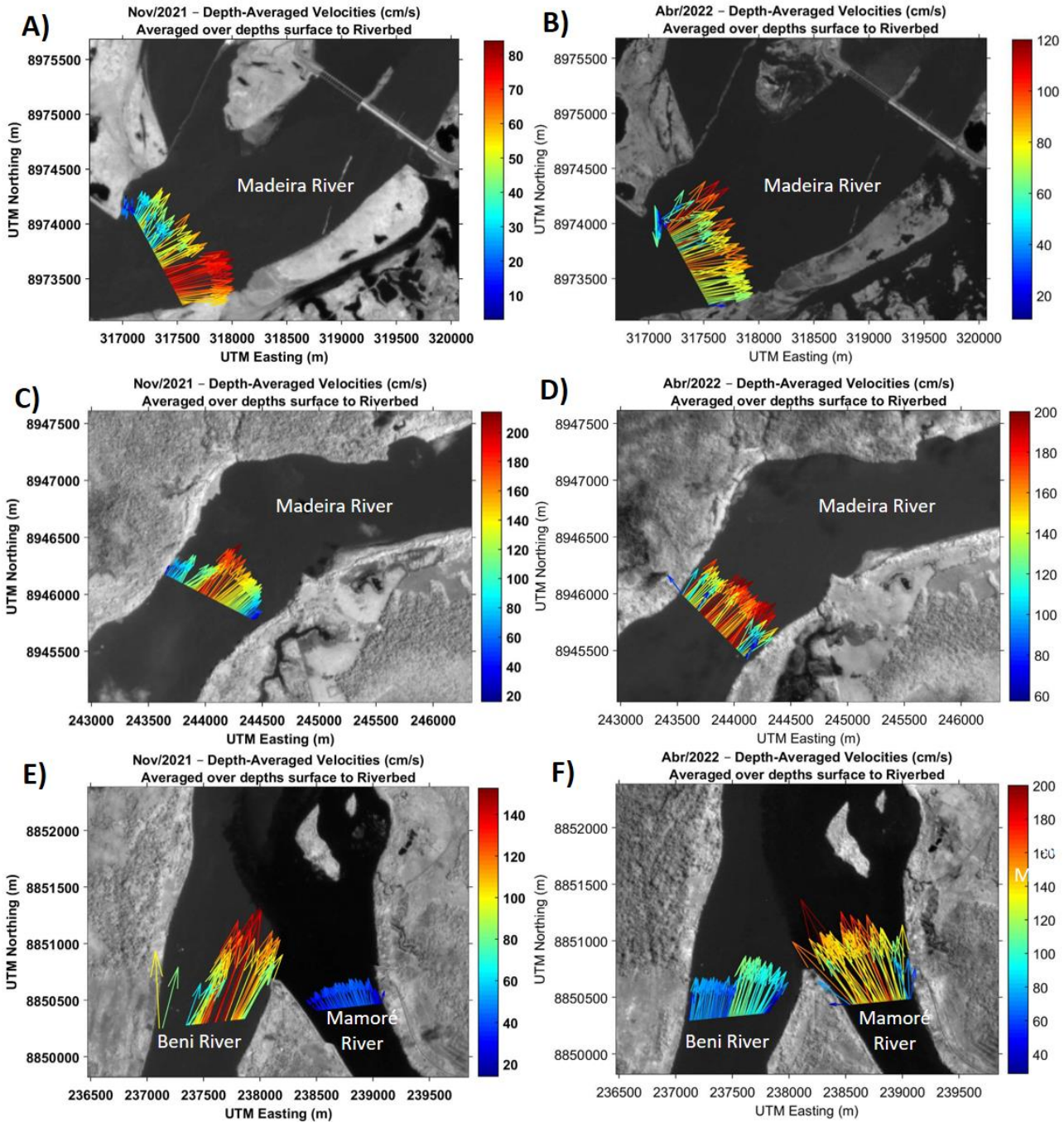

Figure 9. Mean velocity vectors with depth (cm.s^{-1}) and flow direction in the cross-sections of the Madeira River (EST and TAM) and at the Beni–Mamoré confluence, comparing low water (November/2021; panels A, C, E) and high water (April/2022; panels B, D, F).

During the high-water period (April 2022), an increase in mean velocities was recorded in all sections. The EST section showed more intense and better distributed vectors, with a mean of 1.34 m.s^{-1}, reaching maximum values in the center and on the left bank. The TAM section recorded mean velocities of 1.83 m.s^{-1}, maintaining concentration in the center, but with a more homogeneous distribution along the channel. At the Beni-Mamoré confluence, a reversal of the seasonal pattern was observed, with the Mamoré reaching a mean of 1.38 m.s^{-1} and exceeding the Beni (1.10 m.s^{-1}), showing more intense and distributed vectors.

5. Discussion

The hydrosedimentary dynamics at the Beni-Mamoré confluence are conditioned by geological, hydroclimatic, and anthropogenic factors that manifest themselves on distinct temporal and spatial scales. Regional climate variability, characterized by an increase in the frequency of dry days and a reduction in mean annual precipitation after 1991 in the southern portion of the basin (Mamoré River), contrasting with an increase in wet days in the northern portion (Beni River), directly influences sediment transport patterns. (Espinoza et al., 2019).

In this context, the contrasts in suspended sediment concentration (SSC) among the rivers that form the Madeira River can also be interpreted considering differences in the pathways of sediment supply from the Andean piedmont to the monitoring sections. The association between precipitation variability and changes in SSC in the upper Madeira is consistent with results presented for the basin by Rivera et al. (2019, 2021). In the case of the Mamoré River, the presence of extensive floodplains and the foreland region may favor the retention/deposition of some of the material before downstream transfer, contributing to lower mean concentrations compared to the Beni River (Vauchel et al., 2017). The changes in land use and land cover described by Severo e Marinho (2023) provide important context for the recent evolution of the basin landscape but do not, by themselves, explain the observed differences in mean SSC, which reach 639 $mg.L^{-1}$ in the Beni River and 218 $mg.L^{-1}$ in the Mamoré River.

The predominance of Andean sedimentary input, quantified by Guyot, Jouanneau and Wasson, (1999) is reflected in the high specific yield values observed, especially in the BEN section (2.07 $ton.km^{-2}.year^{-1}$). This Andean predominance exerts strong control over fluvial morphodynamics for hundreds of kilometers downstream from the headwater zone, as discussed by Constantine et al. (2014) for large Amazonian rivers.

The suspended material transported by the Madeira River to its mouth comes mainly from the Beni and Mamoré rivers, and the lowland tributaries have little contribution (Espinoza Villar et al., 2013; Filizola e Guyot, 2011; Vauchel et al., 2017). The variations observed reflect both the geomorphological characteristics of the sections and the differences in the seasonal regime of the rivers, highlighting the complexity of the processes that govern the system. On the other hand, large hydropower dam in low-altitude regions can alter the characteristics and river morphology (Timpe; Kaplan, 2017).

In the Madeira River basin, this type of intervention is also discussed in terms of reduction/redistribution of the suspended sediments and geomorphological reorganization associated with the implementation of hydropower dams (Latrubesse et al., 2017; Santos et al., 2024). In addition to basin-scale controls, the patterns observed in the SSC–Q relationship allow us to discuss the temporal response of the hydrosedimentary system throughout the hydrological cycle.

The SSC–Q hysteresis loops allow us to discuss differences between the rising and falling branches and, in general terms, the speed at which SSC responds to variations in Q. Clockwise loops are usually associated with a faster response of suspended sediment, while counterclockwise patterns indicate a later response, with implications for delivery time and relative location of sources (Jing et al., 2025). Since the loops stem from discrete field campaigns, the interpretation is restricted to the observed seasonal pattern, without any intention of characterizing individual events.

Given this, the predominantly clockwise loops in the analyzed sections are consistent with a greater contribution from proximal/rapid mobilizing sources. Furthermore, the linear SSC–Q fits indicated moderate R^2 values in BEN and MAM (0.66–0.67) and lower values in TAM (0.37), consistent with greater dispersion of SSC–Q pairs in TAM. Taken together, the differences in shape, dispersion, and fit between BEN/MAM and TAM/EST suggest combined effects of proximity to the Andean source, lateral storage, and downstream hydraulic control.

The behavior observed in the BEN section, with abrupt reductions in SSC during low water followed by a gradual increase with increased water discharge, is consistent with the dynamics of large tropical rivers described by Latrubesse, Stevaux and Sinha (2005), where seasonal alternations between high and low water levels condition the morphological response of the system. In the TAM and EST sections, the more damped response of SSC in relation to water discharge variation may be associated with the greater distance from the Andean sedimentary source and the influence of downstream hydraulic systems (Charlton, 2008; Chow, 2009; Vanoni, 2006).

The vertical stratification of SSC showed distinct seasonal patterns, being more pronounced during high water in all sections analyzed. During high water, there is greater vertical stratification of sediments, especially in TAM, where the depth/surface ratio reached 3.10. The observed stratification coefficients for BEN (2.9), MAM (4.13), TAM

(3.10) and EST (2.80) significantly exceeded the values of 1.7 recorded by Filizola (2003) in the lower course of the Madeira River, indicating conditions of greater vertical heterogeneity in the studied reach.

This greater vertical stratification of SSC during high water may be related to increased sediment transport from Andean headwater areas, as suggested by Vauchel et al. (2017). The more uniform distribution observed in the Madeira River in the EST section may reflect mixing and deposition processes associated with the local channel morphology and the integration of contributions from the main tributaries, as well as the influence of the reduced channel velocity, which decreases the material transport capacity due to the proximity of the reservoir.

The backscatter patterns of the ADCP signal support direct measurements, although the relationship between signal intensity and sediment concentration is not linear. According to Filizola and Guyot (2004), SSC estimation by backscattering requires specific calibration per stretch, limiting operational applications, but offering potential for complementary monitoring.

In terms of longitudinal balance, the results also indicate losses between the confluence and the downstream section. The 15% sediment deficit observed between the confluence and the EST section represents a continuation of the reduction trend identified by Rivera et al. (2019, 2021), although to a lesser extent than the 36% (Beni) and 30% (Madeira) reductions documented by the authors between 2003-2017. Similarly, Latrubesse et al. (2017) also identified a ~20% reduction in the mean annual surface SSC of the Madeira River downstream of the Santo Antônio dam, in the Porto Velho region, indicating a decrease in the availability/concentration of suspended sediments in the reach under the influence of the Madeira Complex. This reduction may be related to deposition favored by low-energy zones associated with the rectilinear geometry of the channel, which, according to Best and Rhoads (2008), promote recirculation and backwater areas favorable to sediment deposition.

The high specific yield in the Beni River (2.07 ton.km^{-2}.year^{-1}) confirms its dominant role in regional sedimentary dynamics, while the reduced specific yield in the EST section (0.24 ton.km^{-2}.year^{-1}) indicates retention associated with the influence of hydraulic systems, such as the Jirau hydropower dam. This retention favors the deposition of finer particles, as presented by Rivera et al. (2019, 2021) and corroborated by bathymetric data from Cordeiro et al. (2024) and remote sensing data from Santos et al. (2024).

The flow velocity distribution showed strong seasonal asymmetry at the confluence, with the Beni River dominating in low-water (1.10 m.s^{-1} versus 0.25 m.s^{-1} in the Mamoré River) and reversing in high-water, when the Mamoré River surpasses the Beni River (1.38 m.s^{-1} versus 1.10 m.s^{-1} in the Beni River). The Y-shaped (160°) geometry of the confluence limits the mixing of flows and favors recirculation zones (Best, 1987; Best; Rhoads, 2008).

In addition to local hydrodynamic controls, the valley geometry and the presence of meanders upstream of Jirau hydropower dam may favor sediment storage before the narrower reach associated with the EST section. In the upper Madeira River, morphostructural compartmentalization is associated with reaches with narrowing of the floodplain and changes in sinuosity, interpreted in relation to structural barriers/highs, with the potential to alter lateral connectivity and sediment storage in the fluvial corridor (Souza Filho et al., 1999).

In the reach upstream of EST, the wider floodplain and the development of meanders suggest a greater channel-floodplain exchange capacity, which tends to decrease towards the more confined sector. In this context, meandering is important because the increased lateral migration of the channel and the occurrence of meander cutoffs tend to amplify the transfer of sediments from the channel to the floodplain. As meanders migrate and are cutoff, features such as abandoned meanders and new floodplain sectors are formed, which function as areas for sediment accommodation and storage. As a result, some of the transported material can be retained laterally, reducing the fraction that remains in the channel and is exported downstream (Constantine et al., 2014).

In Amazonian rivers with high sediment yield, channel-floodplain exchange and floodplain storage can represent a significant portion of the sediment balance, and the Beni and Mamoré floodplains are described as storage zones (Latrubesse et al., 2017). In the context of dams in the Madeira River, there is evidence of reduced suspended sediments downstream of large hydropower dams and geomorphological control in the location of erosion and siltation areas, reinforcing the need to interpret differences between the reach between TAM and EST monitoring stations considering the floodplain-narrowing contrast and the hydraulic influence of the system (Latrubesse et al., 2017; Santos et al., 2024).

The geomorphological context of the reach, located on the edges of the Amazonian sedimentary basin in contact with the crystalline basement, conditions characteristics of a more incised channel with less relative development of depositional floodplains. This morphostructural configuration limits lateral expansion and

restricts areas of sedimentary storage, predominantly favoring longitudinal transport, in line with the patterns described by Latrubesse (2008) for anabranching rivers in the Amazon. On the other hand, Rivera et al. (2021) emphasize that spatial and temporal variations in precipitation have a direct effect on the concentrations of suspended material in the upper course of the basin.

The comparison with historical data from Guyot et al. (1995) confirms the consistency of the data presented in this work, with similar mean SSC for Beni (690 versus 639 $mg.L^{-1}$) and slightly different values for Mamoré and Madeira, reflecting natural variability and environmental changes in the period between studies. The absolute values of sedimentary transport remain lower than those estimated by Vauchel et al. (2017) due to methodological differences, but confirm the downward trend documented regionally.

5. Conclusions

This study analyzed the hydrosedimentary dynamics at the confluence of the Beni and Mamoré rivers based on field campaigns (2021–2022) and historical series from the HYBAM Observatory, contributing to reducing the information gap on suspended sediment transport in this reach. The results provide insights into the interpretation of hydrosedimentological processes that are essential for the management of the Jirau hydropower dam and the Madeira River waterway.

Significant differences in transport regimes stand out between the analyzed sections. The Beni River presented a higher SSC (639 $mg.L^{-1}$) and sediment specific yield (2.07 $ton.km^{-2}.year^{-1}$) compared to the Mamoré (218 $mg.L^{-1}$ and 0.34 $ton.km^{-2}.year^{-1}$), reflecting their different geological origins and geomorphological conditions. The sections of the Madeira River demonstrated intermediate characteristics with clockwise hysteresis patterns distinct from the rivers that form the Madeira River.

The results of the sediment balance indicate a deficit in sediment transport of approximately 15% between the confluence and the EST section, representing a retention of approximately 40 million tons along 220 km. This retention can be attributed to depositional processes resulting from the reduction in flow velocity in the Madeira River. This type of occurrence is a normal phenomenon when there are significant hydraulic changes in the river system (Charlton, 2008; Chow, 2009; and Vanoni, 2006), such as alterations in the base level of a river, resulting from the construction of hydroelectric dams, for example.

The seasonal and vertical variability of SSC was pronounced, with stratification maxima in high-waters (2.9 in BEN; 4.13 in MAM; 3.10 in TAM; 2.80 in EST), indicating vertical heterogeneity relevant for concentration estimates and for the calculation of sediment flows. The results show a continuation of the trend of reduction in suspended sediment transport documented regionally, although at a lower intensity than in previous periods. The Beni and Mamoré rivers contribute approximately 291 million tons of SSC annually to the Madeira River, confirming their strategic role in the Amazonian sediment balance. The predominance of Andean input and the seasonal patterns of vertical stratification have direct implications for remote sensing estimates and calculations of total sediment flow.

The geomorphological configuration of the confluence (located on the edges of the Amazonian depositional basin) conditions entrenched channel characteristics that limit sedimentary storage areas, favoring longitudinal transport. This configuration, associated with regional hydroclimatic variability and increasing anthropogenic pressures, highlights the need for continuous hydrosedimentary monitoring to support conservation strategies and sustainable use of resources in the basin.

This study contributes to filling gaps in the understanding of the impacts of fluvial regulation on sedimentary regimes in large tropical rivers, providing a scientific basis for future research and environmental management policies in the Amazon. The unprecedented data presented and the proposed hydrosedimentometric balance constitute important tools for the integrated management of water resources in the Madeira River basin in the face of increasing environmental pressures.

Authors Contributions: Conception, E.B.S, R.R.M., J.M., N.P.F. e H.L.R.; methodology, E.B.S, R.R.M., J.M., N.P.F., W.S. e K.A.; validation, E.B.S, R.R.M., J.M., N.P.F., H.L.R, K.A., D.O., A.Z. e O.S.; formal analysis, E.B.S, R.R.M. J.M., H.L.R., W.S., M.S.Q., C.S. e D.F.; investigation, E.B.S., R.R.M., J.M., K.A., D.O., A.Z. e O.S.; resources, J.M., N.P.F., H.L.C., K.A., C.S. e D.F.; curation dos dados, E.B.S. e J.M.; Drafting - initial version, E.B.S., R.R.M., J.M., N.P.F., H.L.R., K.A., W.S., D.O., A.Z., O.S., M.S.Q., C.S. e D.F.; Writing - proofreading and editing, E.B.S., R.R.M., J.M., N.P.F. e M.S.Q.; supervision, R.R.M., J.M., N.P.F., H.L.R. e MSQ;

project management, J.M, N.P.F. e H.L.R.; acquisition of financing, J.M., N.P.F., H.L.C., C.S. e D.F.; All authors have read and agreed with the published version of the manuscript.

Funding: This research was funded by Jirau Energia through the Research and Development Program regulated by the Agência Nacional de Energia Elétrica (ANEEL) (PD-06631-0010/2020).

Acknowledgments: The authors thank the Postgraduate Program in Geography at the Federal University of Amazonas (UFAM). We also thank the H2A research groups and the HYBAM long-term observatory for providing equipment for fieldwork. The authors thank the Fundação de Amparo à Pesquisa do Amazonas (FAPEAM) for the master's level scholarship granted to the first author in the year 2021/2024. We thank the Coordenação de Aperfeiçoamento de Pessoal de Nível Superior – Brazil (CAPES) – funding code 001, and finally, the RBG reviewers for their comments and suggestions that contributed to the final version of the manuscript.

Conflict of Interest: The authors declare a conflict of interest. The funders were involved in the analysis and interpretation of the data, the preparation of the manuscript, and the decision to publish the results.

References

1. ALCÁRCEL-GUTIÉRREZ, F. A.; TAPIAS, J. G.; RAMIÍREZ, N. E. M.; ALMANZA-MELÉNDEZ, M. F. Geological Map of South America in Google Earth. **Journal of Maps**, v. 19, n. 1, p. 1-7, 2023. DOI: 10.1080/17445647.2023.2185167
2. BEST, J. L. FLOW DYNAMICS AT RIVER CHANNEL CONFLUENCES: IMPLICATIONS FOR SEDIMENT TRANSPORT AND BED MORPHOLOGY. In: ETHRIDGE, F. G.; FLORES, R. M.; HARVEY, M. D. (Eds). **Recent Developments in Fluvial Sedimentology**. 1997. p. 27–35.
3. BEST, J. L.; RHOADS, B. L. Sediment Transport, Bed Morphology and the Sedimentology of River Channel Confluences. In: RICE, S. P.; ROY, A. G.; RHOADS, B. L. (Eds.). **River Confluences, Tributaries and the Fluvial Network**. 1. ed. Wiley, 2008. p. 45–72.
4. CHAPMAN, D. **Water Quality Assessments: A guide to the use of biota, sediments and water in environmental monitoring**. Abingdon, UK: Taylor & Francis, 1992.
5. CHARLTON, Ro. **Fundamentals of fluvial geomorphology**. London; New York: Routledge, 2008.
6. CHOW, Ven Te. **Open-channel hydraulics**. Caldwell, NJ: Blackburn Press, 2009.
7. CONSTANTINE, J. A.; DUNNE, T.; AHMED, J.; LEGLEITER, C.; LAZARUS, E. D. Sediment supply as a driver of river meandering and floodplain evolution in the Amazon Basin. **Nature Geoscience**, v. 7, n. 12, p. 899–903, 2014. DOI: 10.1038/ngeo2282
8. CORDEIRO, G. A. R. V.; IANNIRUBERTO, M.; ROIG, H. L.; FERREIRA, O. S.; MARTINEZ, J. M. Seismic assessment of sediment siltation in a tropical run-of-river hydroelectric reservoir. **Environmental Challenges**, v. 16, p. 1-18, 2024. DOI: 10.1016/j.envc.2024.100996
9. DNIT. **Hidrovia do Madeira — Departamento Nacional de Infraestrutura de Transportes**. Disponível em: <https://www.gov.br/dnit/pt-br/assuntos/aquaviario/old/hidrovia-do-madeira>. Acesso em: 27 out. 2023.
10. ESPINOZA, J. C.; SÖRENSSON, A. A.; MOLINA-CARPIO, J.; SEGURA, H.; GUTIERREZ-CORI, O.; RUSCICA, R. CONDOM, T.; WONGCHUIG-CORREA, S. Regional hydro-climatic changes in the Southern Amazon Basin (Upper Madeira Basin) during the 1982–2017 period. **Journal of Hydrology: Regional Studies**, v. 26, p. 1-17, 2019. DOI: 10.1016/j.ejrh.2019.100637
11. ESPINOZA VILLAR, R.; MARTINEZ, J. M.; LE TEXIER, M.; GUOYT, J. L.; FRAIZY, P.; MENESES, P. R.; OLIVEIRA, E. A study of sediment transport in the Madeira River, Brazil, using MODIS remote-sensing images. **Journal of South American Earth Sciences**, v. 44, p. 45–54, 2013. DOI: 10.1016/j.jsames.2012.11.006
12. FILIZOLA, N.. **Transfert sédimentaire actuel par les fleuves amazoniens**. Tese (Doutorado em Hidrologia e Geologia) - U.F.R. Sciences de la Vie et de la Terre, Université Toulouse III Paul Sabatier. 2003. 283P.
13. FILIZOLA, N.; GUYOT, J. L. The use of Doppler technology for suspended sediment discharge determination in the River Amazon / L'utilisation des techniques Doppler pour la détermination du transport solide de l'Amazone. **Hydrological Sciences Journal**, v. 49, n. 1, p. 143–153, 2004. DOI: 10.1623/hysj.49.1.143.53990
14. FILIZOLA, N.; GUYOT, J. L. Fluxo de sedimentos em suspensão nos rios da Amazônia. **Revista Brasileira de Geociências**, v. 41, n. 4, p. 566–576, 2011. DOI: 10.25249/0375-7536.2011414566576
15. GUYOT, J. L.; QUINTANILLA, J; CORTÉS, J.; FILIZOLA, N. Les flux de matières dissoutes et particulaires des Andes de Bolivie vers le río Madeira en Amazonie Brésilienne. **Bulletin de l'Institut français d'études andines**, v. 24, n. 3, p. 415–423, 1995. DOI: 10.3406/bifea.1995.1192

16. GUYOT, J. L.; JOUANNEAU, J. M.; WASSON, J. G. Characterisation of river bed and suspended sediments in the Rio Madeira drainage basin (Bolivian Amazonia). **Journal of South American Earth Sciences**, v. 12, n. 4, p. 401–410, 1999. DOI: 10.1016/S0895-9811(99)00030-9
17. HYBAM. **Observation Service SO HYBAM**. , 2024. Disponível em: <SO-HyBam – Service d'observation des ressources en eaux du bassin de l'Amazone (obs-mip.fr)>. Acesso em: 10 jan. 2023
18. JING, T.; ZENG, Y. FANG, N.; DAI, W.; SHI, Z. A Review of Suspended Sediment Hysteresis. **Water Resources Research**, v. 61, n. 1, p. 1–24, 2025. DOI: 10.1029/2024WR037216
19. LATRUBESSE, E. M. Patterns of anabranching channels: The ultimate end-member adjustment of mega rivers. **Geomorphology**, v. 101, n. 1–2, p. 130–145, 2008. DOI: 10.1016/j.geomorph.2008.05.035
20. LATRUBESSE, E. M.; ARIMA, E. Y.; DUNNE, T.; PARK, E.; BAKER, V. R.; D'HORTA, F.; WIGHT, C.; WITMANN, F.; ZUANON, J.; BAKER, P. A.; RIBAS, C. C.; NORGAARD, R. B.; FILIZOLA JUNIOR, N. P.; ANSAR, A.; FLYVBJERG, B.; STEVAUX, J. C. Damming the rivers of the Amazon basin. **Nature**, v. 546, n. 7658, p. 363–369, 2017. DOI: 10.1038/nature22333
21. LATRUBESSE, E. M.; STEVAUX, J. C.; SINHA, R. Grandes sistemas fluviais tropicais: uma visão geral. **Revista Brasileira de Geomorfologia**, v. 6, n. 1, 2005. DOI: 10.20502/rbg.v6i1.35
22. LI, J.; WANG, G.; SONG, C.; SUN, S. MA, J.; WANG, Y.; GUO, L.; LI, D. Recent intensified erosion and massive sediment deposition in Tibetan Plateau rivers. **Nature Communications**, v. 15, n. 1, p. 722, 2024. DOI: 10.1038/s41467-024-44982-0
23. LOPES, I. M. O.; MAGALHÃES, M. T. Q. Hidrovia do Rio Madeira como indutor de desenvolvimento microrregional das comunidades tradicionais do Baixo Madeira em Porto Velho. **Paranoá: cadernos de arquitetura e urbanismo**, n. 22, p. 143–158, 2018. DOI: 10.18830/issn.1679-0944.n22.2018.10
24. PARSONS, D. R.; JACKSON, P. R.; CZUBA, J. A.; ENGEL, F. L.; RHOADS, B. L.; OBERG, K. A.; BEST, J. L.; MUELLER, D. S.; JOHNSON, K. K.; RILEY, J. D. Velocity Mapping Toolbox (VMT): a processing and visualization suite for moving-vessel ADCP measurements. **Earth Surface Processes and Landforms**, v. 38, n. 11, p. 1244–1260, 2013. DOI: 10.1002/esp.3367
25. QUEIROZ, M. S.; MARINHO, R. R.; CARVALHO, J. A. L.; SILVA, C. F. The geomorphological landscape of the Mariuá Archipelago: An anabranching megacomplex system in the Negro River, Amazon Basin (Brazil). **Geomorphology**, v. 490, p. 1-17, 2025. DOI: 10.1016/j.geomorph.2025.110023
26. RIVERA, I. A.; ARMIJOS, E.; ESPINOZA-VILLAR, R.; ESPINOZA, J.; MOLINA-CARPIO, J.; AYALA, J.; GUTIERREZ-CORI, O.; MARTINEZ, J. M.; FILIZOLA, N. Decline of Fine Suspended Sediments in the Madeira River Basin (2003–2017). **Water**, v. 11, n. 3, p. 1-14, 2019. DOI: 10.3390/w11030514
27. RIVERA, I. A.; MOLINA-CARPIO, J.; ESPINOZA, J. C.; GUTIERREZ-CORI, O.; CERÓN, W. L.; FRAPPART, F.; ARMIJOS, E.; ESPINOZA-VILLAR, R.; AYALA, J. M.; FILIZOLA, N. P. The Role of the Rainfall Variability in the Decline of the Surface Suspended Sediment in the Upper Madeira Basin (2003–2017). **Frontiers in Water**, v. 3, p. 1–14, 2021. DOI: 10.3389/frwa.2021.738527
28. SANTOS, D. R. A.; MARTINEZ, J. M.; OLIVETTI, D.; ZUMAK, A.; GUIMARÃES, D. ANICETO, K.; SEVERO, E.; FERREIRA, O.; HARMEL, T.; CORDEIRO, M.; FILIZOLA, N. SELL, B.; FERNANDES, D.; SOUTO, C.; ROIG, H. Sentinel-2 MSI image time series reveal hydrological and geomorphological control of the sedimentation processes in an Amazonian hydropower dam. **International Journal of Applied Earth Observation and Geoinformation**, v. 128, p. 1–13, 2024. DOI: 10.1016/j.jag.2024.103786
29. SEVERO, E. B.; MARINHO, R. R.; QUEIROZ, M. S.; APOMA, I. ANÁLISE MORFOMÉTRICA DAS BACIAS DOS RIOS BENI E MAMORÉ, BACIA DO RIO MADEIRA. **Margarida Penteado Revista de Geomorfologia**, v. 1, n. 2, p. 1–12, 2024.
30. SEVERO, E. B.; MARINHO, R. R. ANÁLISE DAS MUDANÇAS NA COBERTURA DO SOLO E NA PRECIPITAÇÃO NA BACIA DOS RIOS BENI E MAMORÉ. In: ALEIXO, Natacha Cíntia Regina; DINIZ, Raphael Fernando; VIEIRA, Antonio Fábio Sabbá Guimarães (Eds.). **A GEOGRAFIA AMAZÔNICA EM MÚLTIPLAS ESCALAS**. São Paulo; Manaus: Alexa Cultural; Edua, 2023. v. 3 p. 17–34.
31. SIOLI, H. The Amazon and its main affluents: Hydrography, morphology of the river courses, and river types. *In*: SIOLI, Harald (Ed.). **The Amazon**. Monographiae Biologicae. Dordrecht: Springer Netherlands, 1984. v. 56 p. 127–165.
32. SOUZA FILHO, P. W. M.; QUADROS, M. L. E. S.; SCANDOLARA, J. E.; SILVA FILHO, E. P.; REIS, M. R. COMPARTIMENTAÇÃO MORFOESTRUTURAL E NEOTECTÔNICA DO SISTEMA FLUVIAL GUAPORÉ-MAMORÉ-ALTO MADEIRA, RONDÔNIA-BRASIL. **Revista Brasileira de Geociências**, v. 29, n. 4, p. 469–476, 1999. DOI: 10.25249/0375-7536.1999294469476

33. SOUZA, V. A. S.; ROTUNNO FILHO, O. C.; RODRIGUEZ, D. A.; MOREIRA, D. M.; RUDKE, A. P.; ANDRADE, C. D. Dinâmica da conversão de floresta e tendências climáticas na bacia do rio Madeira. **Ciência Florestal**, v. 32, n. 4, p. 2007–2034, 2022. DOI: 10.5902/1980509865211
34. TIMPE, K.; KAPLAN, D. The changing hydrology of a dammed Amazon. **Science Advances**, v. 3, n. 11, p. 1-13, 2017. DOI: 10.1126/sciadv.1700611
35. VANONI, V. A. **Sedimentation engineering**. 2 ed. Reston, VA: American Society of Civil Engineers, 2006.
36. VAUCHEL, P.; SANTINI, W.; GUOYT, J. L.; MOQUET, J. S.; MARTINEZ, J. M.; ESPINOZA, J. C.; BABY, P. FUERTES, O.; NORIEGA, L.; PUITA, O.; SONDAG, F.; FRAIZY, P.; ARMIJOS, E.; COCHONNEAU, G.; TIMOUK, F.; OLIVEIRA, E.; FILIZOLA, N.; MOLINA-CARPIO, J.; RONCHAIL, J. A reassessment of the suspended sediment load in the Madeira River basin from the Andes of Peru and Bolivia to the Amazon River in Brazil, based on 10 years of data from the HYBAM monitoring programme. **Journal of Hydrology**, v. 553, p. 35–48, 2017. DOI: 10.1016/j.jhydrol.2017.07.018